P2.2 LONGWAVE AND WINDOW ANGULAR DISTRIBUTION MODELS FROM CERES/TRMM RADIANCE MEASUREMENTS

Natividad Manalo-Smtih
Analytical Services and Materials, Inc., Hampton, Virginia

Norman G. Loeb
Center for Atmospheric Research, Hampton University, Hampton, Virginia

1. INTRODUCTION

In order to improve our understanding of the Earth's climate, accurate retrievals of radiant fluxes at the top of the Earth's atmosphere (TOA) are essential. TOA radiant fluxes are inferred from satellite radiance observations by applying angular distribution models (ADMs) which account for the angular variation of the radiation field emerging from a scene. Because of the tremendous variability in Earth scenes, accurate TOA fluxes can only be obtained by accounting for the influence of clear-sky and cloud properties on the radiation anisotropy.

The Clouds and Earth's Radiant Energy System (CERES) [Wielicki,et al.,1996] represents a continuing effort, set forth by its predecessor, the Earth Radiation Budget Experiment (ERBE) [Barkstrom,1984, Smith, et. al.,1986], to produce highly accurate shortwave (SW) and longwave (LW) fluxes at the TOA. The CERES instrument together with the Visible Infrared Scanner (VIRS) aboard the Tropical Rainfall Measuring Mission (TRMM) satellite provide a unique data set for developing ADMs. The CERES instrument package also includes a window (WN) channel in the 8-12 micron region to measure the atmospheric "Greenhouse" effect [Ravel and Ramanathan, 1989]. In addition to scanning in the crosstrack direction, the CERES instrument can also scan in the alongtrack direction and in a rotating azimuth plane scan mode (RAPS), thereby providing multiangle radiance measurements of the same scene. In RAPS mode, CERES scans in elevation as it rotates in azimuth.

In this study, eight months of CERES/TRMM RAPS and alongtrack data from January-August 1998 are used to construct empirical LW and WN ADMs. The ADMs are determined for scene types defined by meteorological and imager-based cloud parameters that influence LW and WN radiance anisotropy. To ensure that there is consistent sampling in all angles for each scene type, the scene types are defined using percentile intervals of these parameters rather than discrete fixed intervals. The ADMs and their sensitivity to the selected parameters are presented.

* *Corresponding Author Address:* Natividad Manalo-Smith, Analytical Services and Materials, Inc. Hampton, VA 23666; e-mail: n.m.smith@larc.nasa.gov

2. THEORY AND IMPLEMENTATION

An instantaneous TOA radiant flux M is estimated from a satellite-measured radiance L as follows:

$$M = \frac{\pi L(\theta)}{R_j(\theta)} \quad (1)$$

where R_j is the anisotropic factor (or ADM) for the "j^{th}" scene type and θ is the viewing zenith angle. R_j is determined as follows:

$$R_j(\theta) = \frac{\pi \bar{L}(\theta)}{M_j} \quad (2)$$

where $\bar{L}_j(\theta)$ is the mean radiance obtained by compositing and averaging all available radiances for each scene type in each θ angular bin, and $\widehat{M}_j$ is determined from:

$$\widehat{M}_j = 2\pi \int_0^{\frac{\pi}{2}} \sin\theta \cos\theta \bar{L}(\theta) d\theta \quad (3)$$

Mean radiances in undersampled angular bins are extrapolated using theoretical model computations.

On TRMM, the CERES scene identification is based on collocated 2-km resolution VIRS measurements over a CERES footprint, which has a 10-km nadir resolution. These radiance measurements, along with VIRS scene information and meteorological and cloud property data, are

recorded on the Single Scanner Footprint TOA/ Surface Fluxes and Clouds (SSF) data product.

As shown in Tables 1 through 3, ADM scene types consist of a combination of surface type, cloud cover and fixed percentile intervals of atmospheric and cloud properties. The vertical temperature change describes the lapse rate in the first 300 mb of the atmosphere above the surface. For cloudy scenes, the cloud emissivity and the cloud-surface temperature difference are area-weighted in the case of multiple layered clouds.

3. RESULTS

The ADMs and their sensitivity to the scene type parameters are illustrated in Figures 1 through 8. The ADMs are represented as a function of viewing zenith angle and in terms of the ADM index *AI*, which is calculated by:

$$AI = \sqrt{\frac{\sum_{i=1}^{n} (R_{ji} - R_{Lamb})^2}{n}} \quad (4)$$

where the ADM index gives an indication of the RMS deviation from a Lambertian case ($R_{Lamb} = 1$) over the range of n view zenith angle bins for a scene type j. Anisotropy increases with ADM index.

Figure 1 shows that the anisotropy for a clear land scene increases as the vertical temperature change increases. The ADMs also exhibits an increase in anisotropy with precipitable water (Figure 2). The clear ocean cases (Figure 3) on the other hand, show little dependence on the vertical temperature change, but show increased limb darkening with precipitable water. A comparison between the day and night desert ADMs is shown on Figures 4 and 5, respectively. Daytime desert ADMs are significantly more anisotropic than the nighttime ADMs due to differences in the daytime and nighttime surface temperatures. Both cases show increased anisotropy with precipitable water. The dependence of overcast ADMs on cloud emissivity and surface-cloud temperature differences is shown in Figures 6 through 8. In general, anisotropy increases as the cloud emissivity decreases, particularly for thin ice clouds (large ΔT and small emissivity in Figure 6), The WN overcast ADM (Figure 8) exhibits a stronger limb darkening than the LW overcast ADMs (Figure 7). Similar results were obtained for other scene types. Examples of anisotropy from broken cloud fields are shown in Figure 9. In that case, ADMs show a large increase in anisotropy with cloud cover.

4. SUMMARY

A new set of angular distribution models have been developed for LW and WN channels from the CERES/TRMM data set. These models are stratified by clear and cloudy sky parameters that affect the anisotropy of Earth scenes.

5. REFERENCES

Barkstrom, B.R. 1984: The Earth Radiation Budget Experiment (ERBE), *Bull. Amer. Meteor. Soc, 65*, 1170-1186.

Ravel, A. and V. Ramanathan, 1989: Observational determination of the greenhouse effect., *Nature,* 342, 758-761.

Smith, G.L., R.N. Green, E. Raschke, L.M. Avis, J.T. Suttles, B.A. Wielicki, and R. Davies, 1986: Inversion Methods for Satellite Studies of the Earth's Radiation Budget: Development of Algorithms for the ERBE mission, *Rev. Geophys., 24,* No.2, 407-421.

Wielicki, B.A., B.R. Barkstrom, E.F. Harrison, R.B. Lee III, G.L.Smith, and J.E.Cooper,1996: Clouds and Earth's Radiant Energy System (CERES): An Earth Observing System experiment, *Bull. Amer. Meteor. Soc., 77*, 853-868.

ADM Category		Scene Type Stratification	Total
CLEAR- %cld<=0.1	Ocean Land Desert	3 Precipitable Water 5 Vertical Temp. Change	45
BROKEN CLOUD FIELD (4 cloud intervals)	Ocean/ Land Desert	3 Precipitable Water 6 T(surface-cloud) 4 IR Emissivity	288(O) 288(L) 288(D)
OVER-CAST	Ocean + Land/ Desert	3 Precipitable Water 7 T(surface-cloud) 6 IR Emissivity	126

Table 1: Preliminary Scene Types for CERES/TRMM LW and WN ADMs.

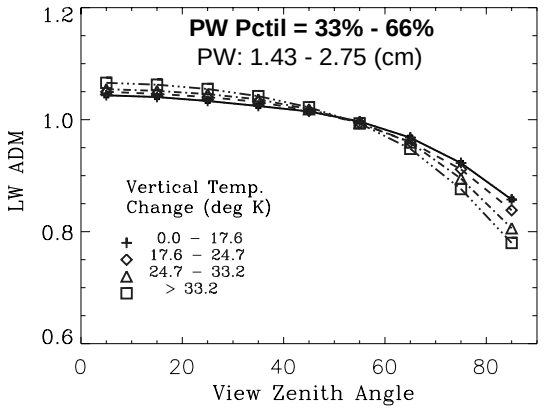

Figure 1. Variation of Clear Sky Land ADM (DAY) with PW and Vertical Temperature Change.

PW Pctile	Broken Cloud Fields			Overcast	
	Cloud Fraction %	ΔT Pctile	Cloud ε Pctile	ΔT (sfc-cld) Pctile	Cloud ε Pctile
< 33	0.1 - 25	ΔT < 0 deg	0 - 25	ΔT < 0 deg	0 -5
		0 -20	25 - 50	0 -20	5 - 10
		20 - 40		20 - 40	10 -25
33 - 66	25 - 50	40 - 60	50 - 75	40 - 60	25 - 50
	50 - 75	60 -80		60 -80	50 -75
> 66		> 80	> 75	80 - 90	> 75%
	75 - 99.9			> 90	

Table 2: ADM Scene Type Parameter Percentile Intervals for Cloudy Scenes.

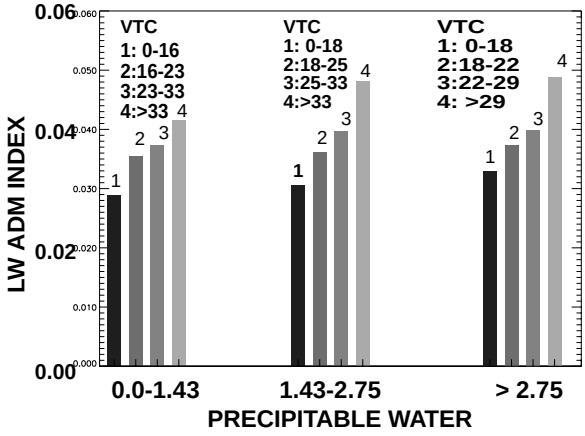

Figure 2. Clear Sky Land LW ADM Index vs. PW and Vertical Temperature Change.

PW Percentile Interval (%)	Vertical Temperature Change Interval (%)
0 - 33	VTC < 0 (deg)
	0- 25
33 - 66	25- 50
	50 - 75
66 - 100	75 -100

Table 3: ADM Scene Type Parameter Percentile Intervals for Clear Sky Scenes.

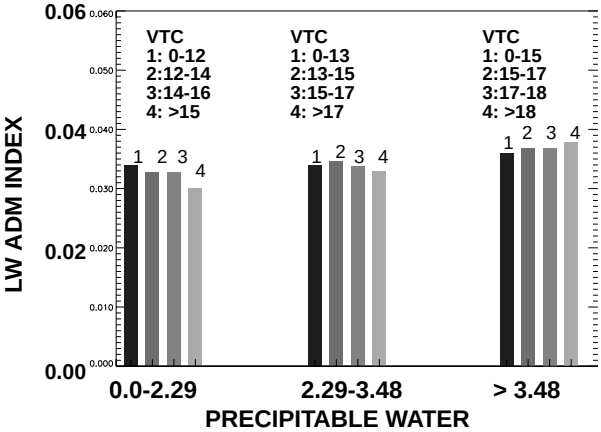

Figure 3. Clear Sky Ocean LW ADM Index vs. PW and Vertical Temperature Change.

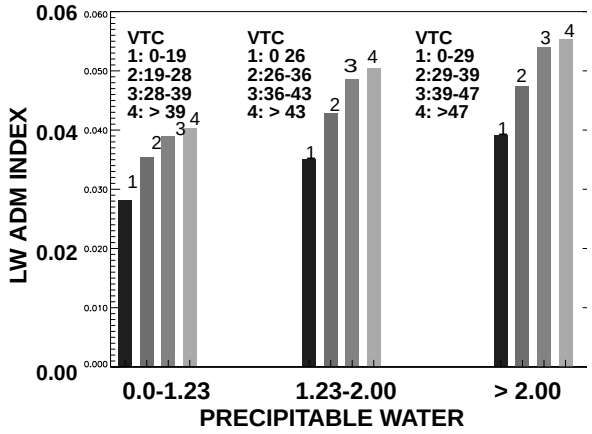

Figure 4. Clear Sky Desert (Day) LW ADM Index vs. PW and Vertical Temperature Change.

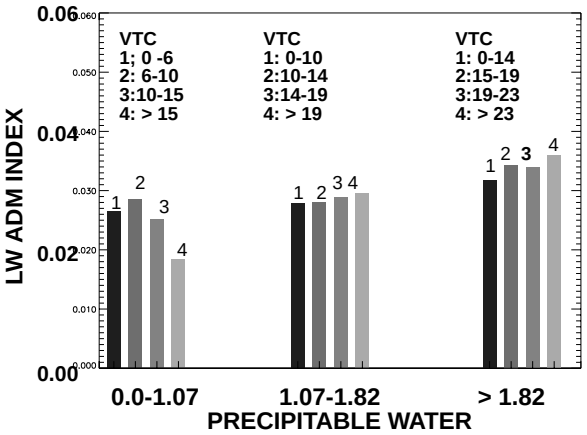

Figure 5. Clear Sky Desert (Night) LW ADM Index vs. PW and Vertical Temperature Change

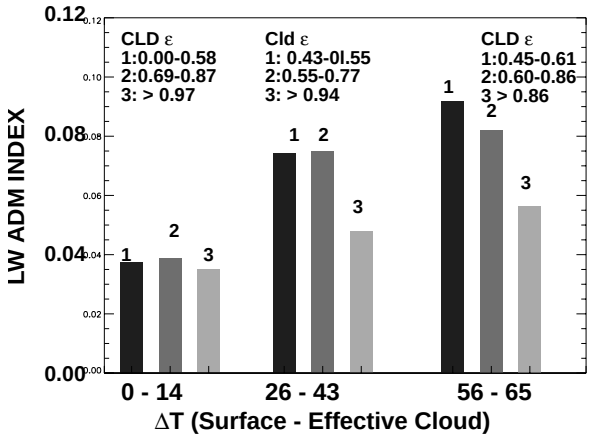

Figure 6. Overcast LW ADM Index vs. Cloud-Surface Temperature Difference and Cloud Emissivity.

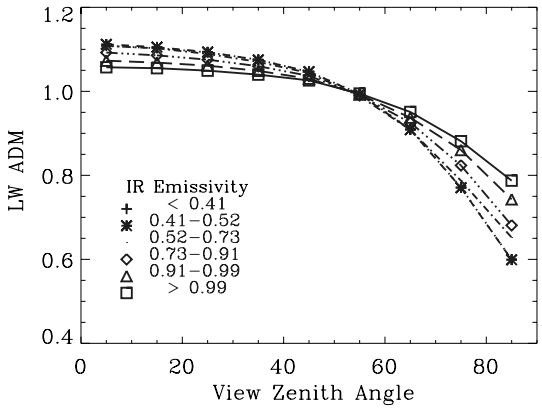

Figure 7. Variation of Overcast LW ADM with cloud emissivity for a given ΔT(33 - 46 K) and PW (> 4.63)

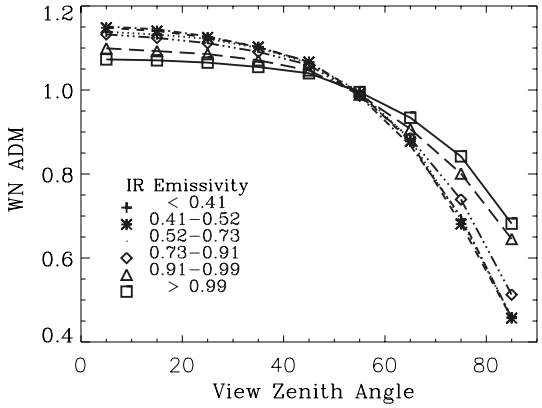

Figure 8. Variation of Overcast WN ADM with cloud emissivity for a given ΔT(33 - 46 K) and PW (> 4.63)

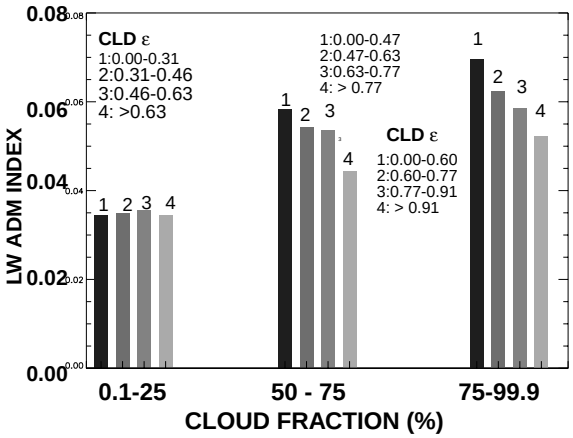

Figure 9. Broken Cloud Field (Land) LDM Index vs. Cloud Emissivity and Cloud Amount.